arXiv:cond-mat/0201253v2 [cond-mat.supr-con] 3 Jun 2002

Structural and Magnetic Instabilities of $La_{2-x}Sr_xCaCu_2O_6$

C. Ulrich[1], S. Kondo[2], M. Reehuis[3], H. He[1], C. Bernhard[1], C. Niedermayer[4], F. Bourée[5], P. Bourges[5], M. Ohl[6], H.M. Rønnow[7], H. Takagi[2] and B. Keimer[1]

[1]*Max-Planck-Institut für Festkörperforschung, Heisenbergstr. 1, D-70569 Stuttgart, Germany*

[2]*Department of Advanced Materials Science, School of Frontier Sciences, University of Tokyo, Hongo 7-3-1, Bunkyo-ku, Tokyo 113-8656, Japan*

[3]*Hahn–Meitner–Institut, Glienicker Str. 100, D-14109 Berlin, Germany*

[4]*Department of Physics, Universität Konstanz, D-78434 Konstanz, Germany*

[5]*Laboratoire León Brillouin, CEA–CNRS, CE Saclay, 91191 Gif sur Yvette, France*

[6]*Institut Laue–Langevin, 156X, 38042 Grenoble Cedex 9, France*

[7]*CEA (MDN/SPSMS/DRFMC), 38054 Grenoble, France*

(March 22, 2022)

Abstract

A neutron scattering study of nonsuperconducting $La_{2-x}Sr_xCaCu_2O_6$ (x=0 and 0.2), a bilayer copper oxide without CuO chains, has revealed an unexpected tetragonal-to-orthorhombic transition with a doping dependent transition temperature. The predominant structural modification below the transition is an in-plane shift of the apical oxygen. In the doped sample, the orthorhombic superstructure is strongly disordered, and a glassy state involving both magnetic and structural degrees of freedom develops at low temperature. The spin correlations are commensurate.

74.25.Jb, 74.25.Ha, 61.2.-q, 74.72.Dn

Typeset using REVTEX

The interplay between ordering phenomena of charge, spin and lattice degrees of freedom has been a focus of recent research on high temperature superconductors. Most of the work has thus far concentrated on two systems: $La_{2-x}Sr_xCuO_4$ (LSCO) and $YBa_2Cu_3O_{6+x}$ (YBCO). In both systems, spin freezing phenomena [1–6] as well as magnetic and structural superlattice formation [7–10] have been observed. The relationship between these effects, some of which were attributed to charge ordering, and anomalies detected by spectroscopic probes (such as the pseudogap and phonon anomalies) is currently an area of very active investigation. As only two compounds have been studied in detail, it has proven difficult to disentangle aspects that are generic to the cuprates from those that are consequences of some non-generic element of the lattice structure of a specific compound. Such elements include the CuO chains in YBCO, and soft optical phonons associated with tilting of the CuO_6 octahedra in LSCO. For instance, charge carriers in the YBCO chains are prone to localization and charge order and may induce related instabilities in the CuO_2 planes. Tilt instabilities of the CuO_6 octahedra, on the other hand, are known to be an important stabilizing factor for static "stripe" order in LSCO and its derivatives [7].

In order to further explore the universality of the structural and electronic instabilities in the cuprates, we have carried out a neutron scattering study of $La_{2-x}Sr_xCaCu_2O_6$ (LSCCO), a compound that crystallizes in a bilayer structure akin to YBCO, but without any electronically active element other than the CuO_2 layers (inset in Fig. 2) [11–13]. Further, tilt instabilities of the kind observed in LSCO are not expected in LSCCO because of the fivefold, pyramidal coordination of copper. LSCCO has thus been termed the simplest bilayer cuprate [11]. We report the discovery of an unexpected low temperature tetragonal-to-orthorhombic transition in undoped and doped LSCCO. In the doped sample, the orthorhombic superstructure does not develop long range order, and the magnetic and structural correlations evolve with temperature in a strikingly parallel manner. Despite the large nominal hole concentration (0.1 holes per Cu), the spin correlations are commensurate.

Single crystals of $La_{2-x}Sr_xCaCu_2O_6$ were grown by the travelling-solvent floating zone method under 1 atm oxygen flow. Most of the measurements were taken on an x=0.2 single

crystal of volume $3 \times 3 \times 3$ mm^3, which is insulating at low temperature, although a metallic behavior of the resistivity is observed at high temperature. (For reasons that are poorly understood at present, superconductivity occurs only in samples treated under high oxygen pressure.) The neutron experiments were carried out on the four-circle diffractometer E5 at the BER II reactor of the Hahn-Meitner-Institut in Berlin, Germany, and on the triple axis spectrometer IN22 at the Institut Laue-Langevin in Grenoble, France. The former instrument was used to acquire a catalogue of Bragg intensities for an accurate refinement of the crystal structure, while the latter instrument allowed us to measure the temperature dependences of selected structural and magnetic reflections with good statistics. On E5, neutron wavelengths of 0.889 Å or 2.36 Å were selected by a copper or a pyrolytic graphite (PG) monochromator, respectively, and the data were collected with a two-dimensional position sensitive ^{3}He-detector. On IN22 the (002) reflection of PG, set for a neutron wavelength of 2.36 Å, was used as both monochromator and analyser, and in order to avoid second order contamination a PG filter was inserted into the incident beam. In order to optimize the intensity, the instrument was used in a focusing mode without collimations.

Two data sets with a total of 623 (259 unique) and 791 (256 unique) reflections were collected on E5 at room temperature and 10 K, respectively. Excellent structure refinements of the room temperature data could be obtained using the tetragonal space group $I4/mmm$. The resulting lattice parameters, atomic coordinates and isotropic temperature factors are listed in Table I and are in good agreement with those of previous reports [11–13]; further details will be reported elsewhere. At 10 K, however, weak additional (and hitherto unobserved) reflections were found, as shown in Fig. 1. Since their intensity increases with increasing momentum transfer Q, these reflections must be attributed to a structural modulation. Their temperature dependence (Fig. 2b) shows that the superstructure develops around 100 K, with diffuse scattering persisting to somewhat higher temperatures.

The superstructure reflections can be indexed as $(h/2,\ k/2,\ l)$ with h, k odd and l even but $\neq 0$, indicating a doubling of the unit cell. From these conditions, the orthorhombic space group $Bmab$ (No. 64, standard setting $Cmca$) with lattice dimensions $a\sqrt{2} \times b\sqrt{2} \times c$

can be deduced. The momentum resolution of our experiment was not sufficient to resolve the small difference between a and b, and for simplicity we continue to use the $I4/mmm$ indexing for the remainder of this article. The atomic coordinates resulting from a refinement of the low temperature data are also given in Table I. The primary difference between the $I4/mmm$ and $Bmab$ structures is a shift of the apical oxygen along the tetragonal (110) direction by ~ 0.05 Å.

The single-layer sister compound LSCO also undergoes a transition from a high temperature tetragonal ($I4/mmm$) to a low temperature orthorhombic ($Bmab$) structure [2], but this transition occurs at a much higher temperature and is commonly believed to be due to steric effects: a mismatch between the natural lattice spacings of the (La/Sr)O and CuO_2 layers is thought to be relieved through a staggered tilt of the CuO_6 octahedra (which involves motions of both in-plane and apical oxygen atoms). In LSCCO, on the other hand, the coordination of copper is fivefold (inset in Fig. 2) and the displacement pattern (Table I) involves almost exclusively the apical oxygen. The origin of the tetragonal-to-orthorhombic transition in LSCCO thus merits some consideration, and as a resistivity minimum occurs for LSCCO samples in this doping range around the same temperature at which the superstructure reflections first appear [14], one may wonder whether the transition could be a consequence of charge localization.

In order to explore this possibility, we have carried out a neutron diffraction study of a Sr-free $La_2CaCu_2O_6$ (LCCO) powder. Although as-prepared LCCO contains a small density of excess oxygen, its resistivity is much larger (and the charge carrier concentration therefore lower) than in LSCCO with x=0.2 [14]. The experiment was carried out on the 3T2 powder diffractometer at the Laboratoire Léon Brillouin in Saclay, France, with a neutron wavelength of 1.2252 Å. While the room temperature data were consistent with previous work [11–13], additional weak structural reflections obeying the same extinction rules as for the x=0.2 compound were again observed at lower temperature (Fig. 2a). The displacement of the apical oxygen is significantly larger than for x=0.2, and the structural transition temperature (170 ± 20 K) is higher.

These data demonstrate the presence of an intrinsic structural instability even without charge carriers, and the enhanced transition temperature in LCCO suggests that the doped carriers suppress the structural phase transition. This is confirmed by considering the widths of the corresponding reflections which are strongly broadened in the x=0.2 sample (Fig. 2c). At low temperature we infer correlation lengths of about ten lattice parameters both in plane and out of plane. Further, the correlation length decreases rapidly as the temperature is increased, which indicates pronounced low energy fluctuations of the corresponding order parameter (that is, the apical oxygen displacement). This result contrasts sharply with the situation in LSCO: While doping-induced *local* structural defects have been reported [15], the orthorhombic superstructure remains long range ordered even in highly doped LSCO. The structural data of Fig. 2c are in fact reminiscent of the rapid evolution of the *magnetic* correlation length with doping and temperature in underdoped LSCO [2].

With this correspondence in mind, we now turn to the magnetic properties of LSCCO. In addition to the orthorhombic superstructure reflections discussed above, Fig. 1 shows that some intensity develops at low temperature around the antiferromagnetic positions $\mathbf{Q} = (1/2,\ 1/2,\ l)$ with l odd. In contrast to the structural reflections, this intensity is only observed at low Q and can hence be identified as magnetic. It also exhibits a sinusoidal intensity modulation as a function of l that extinguishes the $l = 0$ reflection. A similar modulation is observed in antiferromagnetic YBCO and is known to arise from antiferromagnetic interlayer exchange within a bilayer unit [16]. The integrated intensity of a structurally forbidden but magnetically allowed reflection, (1/2, 1/2, 3), is shown in Fig. 3b as a function of temperature. Its onset temperature (~ 90 K) is identical to the structural transition temperature (Fig. 2b) to within the experimental error [17]. The magnetic correlation length is somewhat shorter than that of the orthorhombic superstructure at low temperatures but shows a similar evolution with temperature.

As noted above, this behavior of the magnetic correlation length is characteristic of underdoped LSCO, where the electronic spins are known to freeze out gradually and a spin glass state develops at low temperatures [1–5]. Upon lowering the temperature, manifesta-

tions of magnetic ordering thus appear progressively in neutron scattering and muon spin rotation (μSR) measurements (which are sensitive to fluctuations on meV and μeV energy scales, respectively). In order to complete the description of the microscopic magnetic properties of LSCCO, we have carried out zero-field μSR measurements on the same LSCCO sample studied by neutrons. The experiment was performed at the GPS spectrometer at the Paul-Scherrer-Institute, Switzerland; typical data are shown in the inset to Fig. 3. A gradual onset of muon spin relaxation by slow electronic spin fluctuations is observed upon cooling below 100 K, consistent with the onset of antiferromagnetic diffuse scattering in the neutron experiment (Fig. 3b). However, a precession signal heralding magnetic order that is static on the energy scale set by the muon Larmor frequency only appears at the much lower temperature of 10 K (Fig. 3a). A magnetic anomaly previously found around 10 K in this doping regime [14,18,19] can hence be identified as a spin glass transition. Although the temperature scale is somewhat larger as compared to LSCO, our neutron scattering and μSR data on LSCCO underscore the universality of the spin freezing phenomena for the cuprates.

In summary, we have reported a detailed neutron scattering study of the LSCCO system. The magnetically disordered state we have uncovered is common to the underdoped cuprates. However, the spin correlations found in LSCCO are *commensurate*, whereas *incommensurate* spin correlations are observed in LSCO at comparable Sr concentrations [7,8]. This may either indicate an effective doping level much lower than suggested by the Sr concentration, or it may be a consequence of bilayer interactions; indeed, commensurate quasielastic spin correlations have also been reported in underdoped YBCO [9,10]. Another novel feature of the data presented here is the strongly disordered orthorhombic superstructure in the doped sample. While the substitutional disorder on the La/Ca sites (Table I) may play some role, the broadening originating from such factors is expected to be temperature independent. The parallel temperature evolution of the magnetic and structural order parameters and correlation lengths suggests that structural relaxation of doped holes is the predominant factor inhibiting long range order of both magnetic and lattice degrees of freedom. The

comparison with LSCO is also interesting in this context: LSCCO undergoes its structural transition at a temperature that roughly coincides with the localization of the doped holes, so that structural disorder created by localized holes can effectively frustrate the development of long range order. Charge localization in LSCO, on the other hand, takes place at a temperature at which the orthorhombic superstructure is already well developed, which may explain why the structural manifestations of charge localization are more subtle in that system [15].

As these considerations show, the full implications of our data are yet to be clarified. It is already clear, however, that the characterization of magnetic and lattice superstructures for a lattice type different from those of LSCO and YBCO constitutes an important step in an ongoing effort to develop a comprehensive description of the interplay between spin, charge and lattice degrees of freedom in the cuprates.

REFERENCES

[1] B.J. Sternlieb, G.M. Luke, Y.J. Uemura, T.M. Riseman, J.H. Brewer, P.M. Gehring, K. Yamada, Y. Hidaka and T. Murakami, T.R. Thurston, and R.J. Birgeneau, Phys. Rev. B **41**, 8866 (1990).

[2] B. Keimer, N. Belk, R.J. Birgeneau, A. Cassanho, C.Y. Chen, M. Greven, M.A. Kastner, A. Aharony, Y. Endoh, R.W. Erwin, and G. Shirane, Phys. Rev. B **46**, 14034 (1992).

[3] F.C. Chou, N.R. Belk, M.A. Kastner, R.J. Birgeneau, and A. Aharony, Phys. Rev. Lett. **75**, 2204 (1995).

[4] C. Niedermayer, C. Bernhard, T. Blasius, A. Golnik, A. Moodenbaugh, and J.I. Budnick, Phys. Rev. Lett. **80**, 3843 (1998).

[5] N.J. Curro, P.C. Hammel, B.J. Suh, M. Hücker, B. Büchner, U. Ammerahl, and A. Revcolevschi, Phys. Rev. Lett. **85**, 642 (2000).

[6] J.E. Sonier, J.H. Brewer, R.F. Kiefl, R.I. Miller, G.D. Morris, C.E. Stronach, J.S. Gardner, S.R. Dunsiger, D.A. Bonn, W.N. Hardy, R. Liang, and R.H. Heffner, Science **292**, 1692 (2001).

[7] J.M. Tranquada, N. Ichikawa, and S. Uchida, Phys. Rev. B **59**, 14712 (1999).

[8] Y.S. Lee, R.J. Birgeneau, M.A. Kastner, Y. Endoh, S. Wakimoto, K. Yamada, R.W. Erwin, S.H. Lee, and G. Shirane, Phys. Rev. B **60**, 3643 (1999).

[9] Y. Sidis, C. Ulrich, P. Bourges, C. Bernhard, C. Niedermayer, L.P. Regnault, N.H. Andersen, and B. Keimer, Phys. Rev. Lett. **86**, 4100 (2001).

[10] H.A. Mook, P. Dai, and F. Dogan, Phys. Rev. B **64**, 012502 (2001).

[11] R.J. Cava, B. Batlogg, R.B. Vandover, J.J. Krajewski, J.V. Waszczak, R.M. Fleming, W.F. Peck, L.W. Rupp, P. Marsh, A.C.W.P. James, and L.F. Schneemeyer, Nature **345**, 602 (1990).

[12] H. Shaked, J.D. Jorgensen, B.A. Hunter, R.L. Hitterman, K. Kinoshita, F. Izumi, and T. Kamiyama, Phys. Rev. B **48**, 12941 (1993).

[13] H. Deng, C. Dong, H. Chen, F. Wu, S.L. Jia, J.C. Shen, and Z. X. Zhao, Physica C **313**, 285 (1999).

[14] K. Kinoshita and T. Yamada, Phys. Rev. B **46**, 9116 (1992).

[15] E.S. Bozin, G.H. Kwei, H. Takagi and S.J.L. Billinge, Phys. Rev. Lett. **84**, 5856 (2000).

[16] J.M. Tranquada, G. Shirane, B. Keimer, S. Shamoto and M. Sato, Phys. Rev. B **40**, 4503 (1989).

[17] The (3/2, 3/2, 4) reflection shown in Fig. 2b is both structurally and magnetically allowed, but only about 5 % of its intensity is of magnetic origin.

[18] E.J. Ansaldo, C. Niedermayer, H. Glückler, C.E. Stronach, T.M. Riseman, D.R. Noakes, X. Obradors, A. Fuertes, J.M. Navarro, P. Gomez, N. Casan, B. Martinez, F. Perez, J. Rodriguez-Carvajal, R.S. Cary, and K. Chow, Phys. Rev. B **46**, 3084 (1992).

[19] I. Felner, D. Hechel, E.R. Yacoby, G. Hilscher, T. Holubar, and G. Schaudy, Phys. Rev. B **47**, 12190 (1993).

TABLES

TABLE I. Positional parameters of $La_{1.8}Sr_{0.2}CaCu_2O_6$ at 10 K and 295 K from single–crystal neutron diffraction. For the refinements of the 10 K data the occupancies of the atoms were taken from refinements of the tetragonal structure and were not allowed to vary. La/Sr and Ca are partially exchanged, and by taking the different multiplicities of the Wyckoff positions into account we obtain the formula $[(La/Sr)_{1.81}Ca_{0.19}][Ca_{0.83}(La/Sr)_{0.17}]Cu_2O_6$. Because the ionic radii of La^{3+} and Sr^{2+} are similar, we expect a La:Sr ratio of 9:1 on each position.

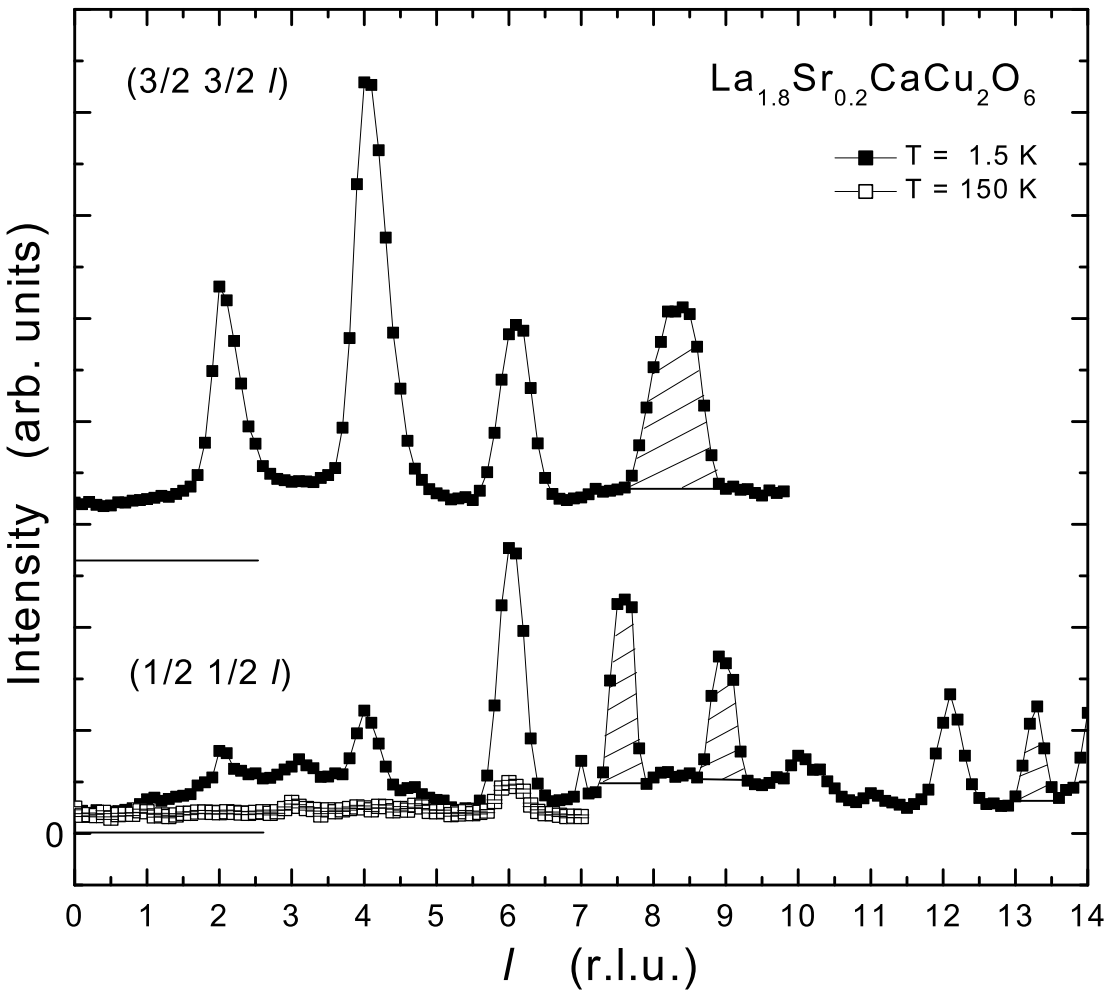
Atom		x	y	z	B_{iso} [Å^2]	*Pop*
at 295 K	$I4/mmm$	$a = b = 3.7974(4)$ Å, $c = 19.3138(19)$ Å				
La/Sr	4*e*	0	0	0.17600(9)	0.58(4)	0.90(3)
Ca	4*e*	0	0	0.17600	0.58	0.10(3)
Ca	2*a*	0	0	0	0.61(8)	0.83(3)
La/Sr	2*a*	0	0	0	0.61	0.17(3)
Cu	4*e*	0	0	0.41447(9)	0.56(3)	1.0
O1	8*g*	0.25	0.25	0.08203(8)	0.82(5)	1.000(14)
O2	4*e*	0	0	0.29639(14)	1.86(9)	1.012(17)
at 10 K	*Bmab*	$a = b = 5.3621(5)$ Å, $c = 19.2436(19)$ Å				
La/Sr	8*f*	0	-0.0009(3)	0.17575(11)	0.42(4)	0.90
Ca	8*f*	0	-0.0009	0.17575	0.42	0.10
Ca	4*a*	0	0	0	0.50(9)	0.83
La/Sr	4*a*	0	0	0	0.50	0.17
Cu	8*f*	0	0.0002(3)	0.41474(11)	0.47(5)	1.00
O1	8*g*	0.25	0.25	0.0831(4)	0.65(7)	1.00
O1’	8*g*	0.25	0.25	0.9183(4)	0.65(7)	1.00
O2	8*f*	0	0.0094(5)	0.29634(17)	1.42(9)	1.01

FIGURES

FIG. 1. Elastic scans along $Q = (0.5, 0.5, l)$ and $(1.5, 1.5, l)$ at 1.6 K and 150 K in the doped $La_{1.8}Sr_{0.2}CaCu_2O_6$ single crystal, showing superstructure reflections at (h/2, k/2, l). The wave vector Q is given in reciprocal lattice units (r.l.u.) based on the lattice parameters of Table I. The intensity for odd l decreases with increasing Q and is thus of magnetic origin. The intensity for even values of l increases with increasing Q and is thus predominantly of structural origin. Diffraction peaks originating from the Al sample holder are marked.

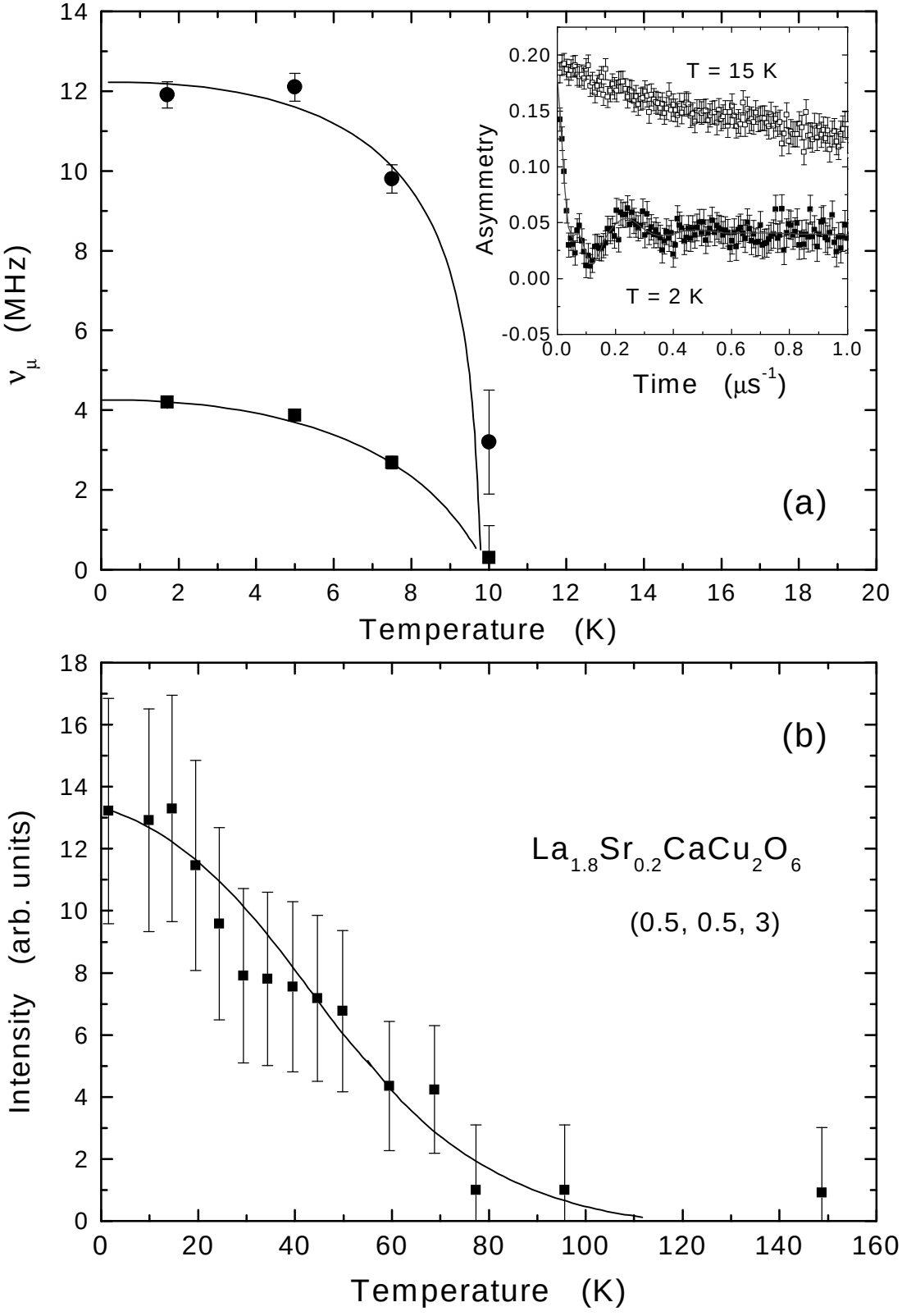
FIG. 2. a) Integrated intensity of the orthorhombic superstructure reflection (3/2, 3/2, 4) of the undoped $La_2CaCu_2O_6$ powder sample and b) of the doped $La_{1.8}Sr_{0.2}CaCu_2O_6$ single crystal as a function of temperature. Panel c shows the temperature dependence of the intrinsic full width at half maximum (FWHM) of the (3/2, 3/2, 4) peak measured along $(h, h, 0)$ in the doped compound. The lines are guides-to-the-eye. The inset displays the unit cell at T = 295 K. The CuO_5 pyramids are highlighted. (The Cu atoms at the center of the pyramid base are not shown for clarity.)

FIG. 3. a) Temperature dependence of the zero-field μSR Lamor frequencies measured in the $La_{1.8}Sr_{0.2}CaCu_2O_6$ single crystal. The two distinct frequencies indicate two inequivalent muon sites. The inset displays the asymmetry versus time spectrum for two different temperatures above and below the magnetic ordering temperature. The lines are guides-to-the-eye. b) Temperature dependence of the integrated intensity of the (1/2, 1/2, 3) reflection measured by neutron scattering.


(3/2 3/2 l)
La1.8Sr0.2CaCu2O6
T = 1.5 K
T = 150 K
(1/2 1/2 l)
Intensity (arb. units)
0
0 1 2 3 4 5 6 7 8 9 10 11 12 13 14
l (r.l.u.)

This figure "fig2.gif" is available in "gif" format from:

http://arxiv.org/ps/cond-mat/0201253v2


(a)
ν_μ (MHz)
Temperature (K)
Asymmetry
T = 15 K
T = 2 K
Time (μs^{-1})
(b)
$La_{1.8}Sr_{0.2}CaCu_2O_6$
(0.5, 0.5, 3)
Intensity (arb. units)
Temperature (K)